ELSEVIER

Chemical Engineering Journal 132 (2007) 335–343

Chemical Engineering Journal

www.elsevier.com/locate/cej

Production of glass-ceramics obtained from industrial wastes by means of controlled nucleation and crystallization

M. Erol *, S. Küçükbayrak, A. Ersoy-Meriçboyu

Department of Chemical Engineering, Chemical & Metallurgical Engineering Faculty, Istanbul, Technical University, Maslak 34469, Istanbul, Turkey

Received 10 November 2006; received in revised form 11 January 2007; accepted 23 January 2007

Abstract

Glass-ceramic materials were produced from coal fly ashes obtained from Tunçbilek and Orhaneli thermal power plants in Turkey without or with the addition of red mud from aluminum production and silica fume. The nucleation and crystallization experiments were carried out on the basis of differential thermal analysis (DTA) results to produce glass-ceramic materials. X-ray diffraction (XRD) analysis of the produced glass-ceramic materials revealed that the main crystalline phases were diopside ($Ca(Mg,Al)(Si,Al)_2O_6$) and aluminum augite ($Ca(Mg,Fe^{3+},Al)(Si,Al)_2O_6$). The microstructure of the glass-ceramic materials was examined by scanning electron microscopy (SEM). Microstructural observation clearly indicated that the crystallization volume increased when the length of thermal treatment time increased. Glass-ceramic samples produced from industrial wastes had high density and microhardness values with a zero porosity and negligible water adsorption. Toxicity characteristic leaching procedure (TCLP) results showed that the produced glass-ceramic samples are non-toxic materials. Glass-ceramic sample showed high resistance to alkali solutions in contrast to acidic solutions. Overall results indicated that the glass-ceramic samples produced from waste materials with several desirable properties that would make them attractive to industrial use in construction, tiling and cladding applications.

Keywords: Coal fly ash; Waste recycling; Glass-ceramic

1. Introduction

In the near future the development of new recycling technologies is getting more important and the recycling of by-products and industrial waste materials will dramatically increase. Fly ash, a waste product of coal combustion in thermal power plants, is produced in dry form in large quantities and thus is a major source for environmental pollution. Currently, large quantities of fly ash are used for landfilling which cause negative environmental impacts such as leaching of potentially toxic substances into soils and groundwater, the change in the elemental composition of the vegetation growing in the vicinity of the ash and the accumulation of toxic elements throughout the food chain [1]. Therefore, it is necessary for the inertization of fly ashes, to look for new technologies in order to immobilize their dangerous components in glass and glass-ceramic materials.

Coal fly ash contains large amounts of SiO_2, Al_2O_3, CaO which are main glass network formers, therefore it can be a good candidate for the glass-ceramic production as a raw material source. In recent years, production of glass and glass-ceramic materials from industrial wastes such as coal fly ash, incinerator fly ash and steel fly ash [2–5] have been paid much attention to make them reasonably safe for the environment. The recycling of industrial wastes in glass-ceramic production is an effective way for the volume reduction of the wastes and the immobilization of the heavy metals.

Glass-ceramics are polycrystalline materials produced by controlled crystallization of suitable glasses during specific heat treatment processes. The glass-ceramic production process comprises the preparation of a homogeneous glass, the shaping of the glass to produce the required articles and finally the application of a controlled heat treatment process. Controlled heat treatment consists of two steps: nucleation and crystal growth [6]. In the nucleation stage, glass is heated to the maximum nucleation temperature and held for a sufficient time for stable nuclei formation. Following nucleation, the temperature is raised to the crystallization temperature and held at that temperature

* Corresponding author. Tel.: +90 212 285 3351; fax: +90 212 285 2925.
E-mail address: erolm@itu.edu.tr (M. Erol).

1385-8947/$ – see front matter © 2007 Elsevier B.V. All rights reserved.
doi:10.1016/j.cej.2007.01.029

Table 1
Chemical analysis of fly ash samples [8,9]

Waste materials	SiO_2 (%)	Al_2O_3 (%)	CaO (%)	MgO (%)	Fe_2O_3 (%)	Na_2O (%)	K_2O (%)	SO_3 (%)	LOI[a] (%)
Tunçbilek fly ash	54.08	25.58	3.10	3.03	9.82	0.58	1.51	0.22	2.01
Orhaneli fly ash	32.83	13.34	30.35	4.51	5.61	2.15	1.37	5.85	3.67
Silica fume	90.80	1.02	2.55	0.94	1.93	–	–	0.50	1.57
Red mud	10.40	28.50	3.90	7.70	35.1	3.80	1.60	4.65	3.90

[a] LOI: loss of ignition.

for a selected period of time, where the crystal growth occurs. The nucleation and crystallization of glasses are important in understanding the stability of glasses in practical applications and in preparing glass-ceramics with desired microstructures and properties [7].

Initial composition and the heat treatment conditions are the most important parameters that effect the kind of crystalline phases occurred in the glass-ceramics and the final properties of the materials. Glass-ceramics possessing desirable properties to fulfill many applications can be produced from waste materials by applying suitable heat treatments. Glass-ceramics based on wastes can have different applications, such as wall-covering panels, floors and roofs in industrial and public buildings, interior facing of containers for the chemical industry and as road surfacing [2].

The present research concentrate on the production of glass-ceramic materials from coal fly ashes obtained from Tunçbilek and Orhaneli thermal power plants in Turkey, red mud from aluminum production and silica fume in order to reduce the waste materials' volume, make them more inert and to produce a new marketable product useful in the construction industry.

2. Experimental procedure

2.1. Starting material

The raw materials used in this study were coal fly ashes obtained from Tunçbilek and Orhaneli thermal power plants in Turkey, red mud from aluminum production and silica fume. Chemical compositions of the waste samples were given in Table 1 [8,9] and the ICP test results of heavy metals in the waste materials were summarized in Table 2.

It is clear that the major chemical components in fly ash samples are SiO_2, Al_2O_3 and CaO. The total amount of SiO_2–Al_2O_3–CaO varied in the range of 76.52–82.76%. The chemical composition of Tunçbilek fly ash sample is typical of the most common glassy ternary systems. Significant amount of Fe_2O_3, which can be used as a nucleating agent, is also present especially in the Tunçbilek fly ash sample. The SiO_2, Al_2O_3 and Fe_2O_3 contents of the Orhaneli fly ash is low while it has significant amount of CaO compare to Tunçbilek fly ash sample. Red mud and silica fume were composed of mostly Fe_2O_3 and SiO_2, respectively. They were used as additives in Orhaneli fly ash batch. All other elements such as Cr, Mn, Zn and Pb were determined in the parts per million range (Table 2).

Table 2
Heavy metals detected in fly ash samples

Waste materials	Cr^{3+} (ppm)	Mn^{2+} (ppm)	Zn^{2+} (ppm)	Pb^{2+} (ppm)
Tunçbilek fly ash	20.30	11.70	10.50	28.70
Orhaneli fly ash	14.70	9.20	7.90	21.40
Silica fume	10.23	5.62	4.23	11.21
Red mud	19.21	13.23	10.21	28.24

2.2. Glass preparation and heat treatment

Glass samples were prepared from the fly ashes without or with the addition of red mud and silica fume. In each batch 20 g of fly ash was melted in platinum crucible for 2 h in an electrically heated furnace at 1773 K. To ensure homogeneity, the melt was poured into water. The cast glasses were crushed, pulverized and remelted at the same temperature for 3 h to remove the air bubbles from the melt. Following this procedure, the refined melt was cast in a preheated graphite mould (673 K) to form cylinders of approximately 0.8–1 cm in diameter and 1–4 cm in length. The cylinders were cooled to room temperature. To remove thermal residual stress, the cast glasses were annealed in a furnace at 873 K for 2 h followed by slow cooling to room temperature. The annealing temperature and time were chosen on the basis of the results obtained in a previous study [10].

2.3. Differential thermal analysis and heat treatment

DTA scans of annealed glass specimens were carried out using Rigaku (Model Thermoflex) thermal analyzer to detect the glass transition (T_g) and the crystallization peak temperatures (T_p). DTA was connected to a computer. All peak temperatures and peak heights were determined by using a software program. DTA experiments were performed by heating 20 mg glass samples in a Pt-crucible and using Al_2O_3 as a reference material in the temperature range between 293 and 1373 K. DTA measurements were applied to the produced glass samples to determine the glass transition temperature (T_g), the maximum nucleation temperature, maximum nucleation time and crystallization temperature at a heating rate of 10 K/min. For the determination of the maximum nucleation temperature, the as-quenched glass samples were held for 4 h at different nucleation temperatures that is above the T_g, in 5 K intervals. To estimate the maximum nucleation time, the glass samples were heat treated isothermally at the maximum nucleation temperature for 1, 2, 3 and 4 h.

To produce the glass-ceramic samples, classical method was applied to the bulk glass samples. For this purpose, produced glasses were cut by diamond saw blade in identical pieces with a disc shape of about 10 mm diameter and 5 mm height suitable

for microstructural and mechanical characterizations. Then the glass samples were crystallized by suitable nucleation and crystal growth heat treatments on the basis of DTA results. For this purpose, glass samples were placed in an alumina brick and heated at a rate of 10 K/min to the maximum nucleation temperature and held at this temperature for maximum nucleation time. Following the nucleation, the temperature was raised to the crystallization temperature and held at this temperature for 15, 30 and 60 min to examine the effects of holding time at the crystallization stage on the microstructural, mechanical, physical, and chemical properties of the produced glass-ceramic samples. The crystallized samples were then cooled in the furnace. Heat treatments were carried out in an electric muffle furnace.

2.4. X-ray diffraction studies

X-ray diffraction was utilized to estimate which crystalline phases occurred in the produced samples and also to determine if the sample had fully crystallized.

In all cases, samples which were analyzed by X-ray diffraction were ground to fine powder form. A Siemens diffractometer Model D 5000 operated at 40 kV and 30 mA utilizing Cu Kα radiation was used for the measurements. The detector was scanned over a range of 2θ angles from 10° to 80°, at a step size of 0.02° and a dwell time of 2 s per step. The resulting powder diffraction patterns were analyzed utilizing a software package program.

2.5. Scanning electron microscopy analysis

SEM investigations were conducted in an Amray Model 1830 operated at 20 kV to observe the microstructure of the produced samples. Samples were mounted (using Buehler Model Simpliment II) in epoxy resin and their surfaces were ground flat by 400, 800, 1000 and 1200 grit abrasive paper. Then the samples were polished with diamond paste to achieve a mirror-smooth surface. The polished samples were etched with HF solution (5 vol.%) for 1.5 min, immediately rinsed with excess distilled water and then cleaned in ethanol for 2 min. The samples were coated with carbon prior to examination. The microstructures of the samples were examined by SEM and the photographs were taken. The volume and aspect ratio of crystals occurred in the microstructure of the glass-ceramic samples were determined with the aid of an image analyzer from SEM micrographs.

2.6. Measurements of the density, porosity and mechanical properties

Vickers microhardness measurements were done on the produced glass-ceramic samples. The microhardness tester used in this study was a Leco Model M-400-G. Samples were ground and polished with diamond paste. A load of 0.5 kg was selected and the time of indentation was fixed as 15 s. In order to obtain reliable statistical data, at least 15 indentations were made on each sample. The size of the indentation was precisely measured with a microscope having a good resolving power.

Density and the porosity of the produced glass-ceramic samples were measured by using a Quantachrome Autoscan-33 mercury porosimeter. Mercury intrusion porosimetry measurements of the samples were carried out pressurizing the system up to 227 MPa with a Hg contact angle of 140°. Data on density and percent porosity were acquired through a microcomputer data acquisition system interfaced with the porosimeter.

2.7. Toxicity characteristic leaching procedure

Toxicity evaluation was made by application of standard leaching procedures. Leaching test methods are used in order to asses: (i) whether a waste should be classified as hazardous, (ii) the waste treatment process effectiveness and (iii) whether land disposal of a specific waste is an appropriate method of management.

In order to assess the stabilization of the wastes into the glass-ceramic materials, the produced samples were subjected to toxicity characteristic leaching procedure test [11].

A leaching solution (extraction fluid) was used in the TCLP experiments. Extraction fluid consists of 5.7 ml of acetic acid diluted in 500 ml of distilled water, in which 64.3 ml of NaOH (1N) was added and the resulting solution was diluted with distilled water to the volume of 1:l giving a final pH value of 4.93 ± 0.05. The produced samples were manually crushed (<9.5 mm) and placed in a conical flask. Extraction fluid was added in order to keep a liquid to solid ratio of 20 (L/S = 20). The flask is tightly closed and stored at 298 K for 18 h. The resultant solutions were filtered through a 0.6–0.8 μm filter and the concentrations of heavy metals in the leachate were determined by using ICP. A Perkin-Elmer Model Optima 3000 XL ICP operated at 13.56 MHz (using Ar and N_2 gases) was used for the measurements.

2.8. Determination of the chemical resistance and water adsorption of the produced materials

The chemical resistances of the glass-ceramic samples were tested in 10% HNO_3 and 10% NaOH solutions. In these experiments, 2 g of grained samples with average particle sizes between 0.3 and 0.5 mm were treated at 373 K for 2 h in 70 ml solutions. After washing and drying, the ground samples were weighed and the percentages of weight losses were calculated.

The water adsorption (%) of the produced materials was determined using the procedure outlined in the ASTM standards [12].

3. Results and discussions

3.1. Differential thermal analysis and glass production

Differential thermal analysis investigations were carried out on as-cast glass samples to determine the nucleation and crystallization temperatures used in producing a glass-ceramic sample with optimum properties. Fig. 1 shows the DTA thermogram of the glass sample produced from Tunçbilek fly ash scanned at the heating rate of 10 K/min. It can be seen

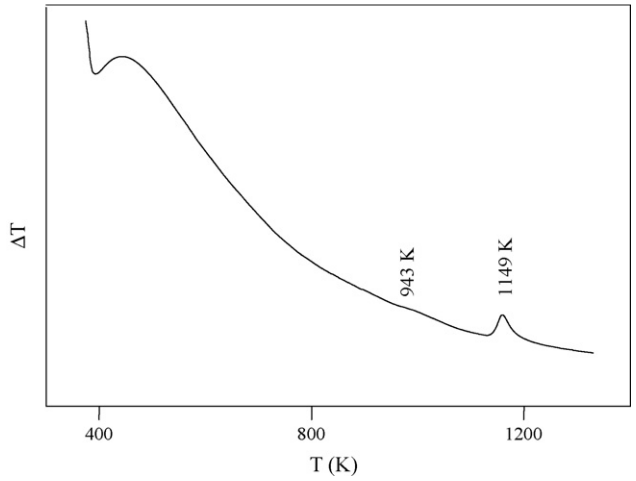

Fig. 1. DTA graph of the Tunçbilek glass (TG) sample.

from Fig. 1 that there were one shallow endothermic peak at 943 K, which shows the glass transition temperature and one exothermic peak at 1149 K corresponding to the crystallization temperature.

DTA result of the glass sample produced from Orhaneli fly ash was given in a previous study [13]. According to the previous study, there was a shallow endothermic peak at 1003 K corresponding to T_g. However, any exothermic peak was not observed in the DTA graph of the glass sample produced from Orhaneli fly ash. According to DTA results, it can be said that glass sample obtained from Tunçbilek fly ash is suitable for the glass-ceramic production and glass-ceramic sample cannot be produced from Orhaneli fly ash without any additives. Therefore, 20% red mud to increase the ratio of Fe_2O_3 (as a nucleating agent) and 20% silica fume to increase the ratio of SiO_2 were added to the Orhaneli fly ash to change the composition of it for suitable glass-ceramic production. DTA experiment was performed on 20 mg of the glass sample produced from Orhaneli fly ash, silica fume and red mud at a heating rate of 10 K/min. The observed DTA graph was given in Fig. 2. As it was seen from Fig. 2, one shallow endothermic peak at 978 K, which shows the glass transition temperature and one exothermic peak corresponding to the formation of a crystalline phase at 1222 K were determined.

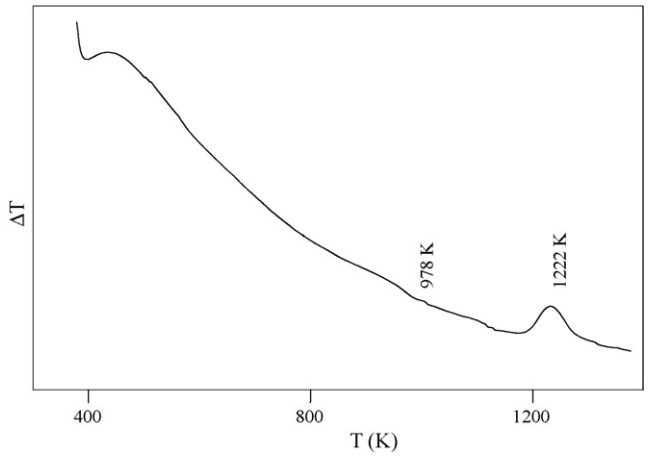

Fig. 2. DTA graph of the Orhaneli glass (ORSG) sample.

TG code was given to the glass produced from Tunçbilek fly ash while the ORSG code was given to the glass produced from Orhaneli fly ash, red mud and silica fume.

3.2. Determination of maximum nucleation temperature and time

As reported by Xu et al. [7], the DTA technique can be used to determine the maximum nucleation temperature and time. In the DTA technique, the crystallization peak temperature, T_p, is determined as a function of the nucleation temperature, T_n, using a constant sample weight and heating rate. The crystallization peak in the DTA occurs because of the heat evolved during crystal growth from the nuclei present in the glass. Any change in DTA peaks for the glass samples nucleated at different temperatures for the same time should result solely from the contribution of N, the number of nuclei. N is proportional to the nucleation rate (I) at the temperature for nucleation (T_n) [14]. For glasses with the same composition, the following relationship [7] is applied between the number of nuclei, N and the crystallization peak temperature, T_p, when the heating rates are the same for the DTA runs (E is the activation energy and R is the gas constant):

$$\ln N = \frac{E}{R}\frac{1}{T_p} + \text{constant} \quad (1)$$

Thus, the greater the number of nuclei, the lower the crystallization temperature. Therefore, the change in T_p with T_n is primarily due to a change in the glass [15]. The height of the crystallization peak, $(\delta T)_p$, is also proportional to N. Although no definite relationship has been established between $(\delta T)_p$ and N, experimental studies [2,16] showed that the concentration of nuclei in the glass increases with the increase in $(\delta T)_p$. For the determination of maximum nucleation temperature, the glass samples were held for 4 h at different nucleation temperatures that is above the glass transition temperature, T_g, in 5 K intervals. To estimate the maximum nucleation time glass samples were heat treated isothermally at the maximum nucleation temperature for 1, 2, 3 and 4 h. The obtained T_p and $(\delta T)_p$ values for all glass samples were summarized in Tables 3 and 4.

Table 3
T_p and $\delta(T)_p$ values of ORSG sample

Nucleation temperature (K)	Holding time (h)	T_p (K)	$\delta(T)_p$
T_p and $\delta(T)_p$ values for different nucleation temperatures			
978	4	1188	0.714
983	4	1185	0.725
988	4	1183	0.753
993	4	1192	0.614
T_p and $\delta(T)_p$ values for different holding times at 988 K			
988	1	1187	0.718
988	2	1178	0.794
988	3	1180	0.773
988	4	1183	0.753

Table 4
T_p and $\delta(T)_p$ values of TG sample

Nucleation temperature (K)	Holding time (h)	T_p (K)	$\delta(T)_p$
T_p and $\delta(T)_p$ values for different nucleation temperatures			
943	4	1138	0.654
948	4	1136	0.669
953	4	1141	0.646
958	4	1142	0.634
T_p and $\delta(T)_p$ values for different holding times at 948 K			
948	1	1143	0.621
948	2	1130	0.706
948	3	1134	0.682
948	4	1136	0.669

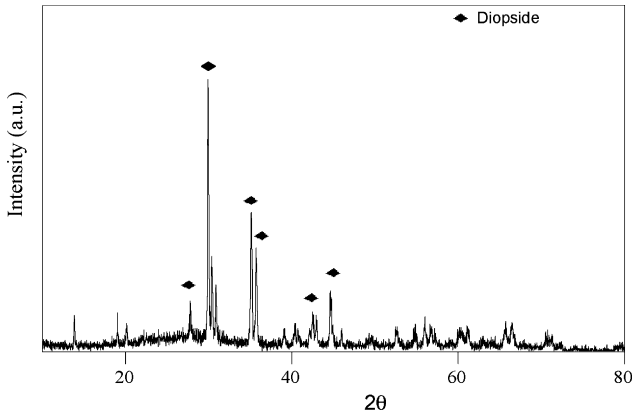

Fig. 3. XRD pattern of the ORSGC-15 sample.

It is well known that the nucleation rate (number of nuclei formed per unit volume per second) is a function of temperature and becomes maximum at a temperature near the middle of the temperature range where nucleation can occur. As seen from Table 3, T_p values reached the lowest value at 988 K while $\delta(T)_p$ values reached a maximum at this temperature for ORSG glass. Therefore, maximum nucleation temperature was selected as 988 K. As seen in Table 3, T_p values decreased and $\delta(T)_p$ values increase until the nucleation time reached 2 h. With increasing time (below 2 h) at the nucleation temperature (988 K), the concentration of nuclei in the glass increases, which increases the crystallization rate during DTA as indicated by the larger $\delta(T)_p$ and lower T_p. The increase in $\delta(T)_p$ and decrease in T_p, which are considered to be the direct result of increasing concentration of nuclei in the glass, are expected to continue until the glass becomes saturated with nuclei. If the crystallization temperature does not vary with the nucleation time, this case shows that the nucleation stage is fully completed [7]. With the increasing of nucleation time, $\delta(T)_p$ values reached a maximum at 2 h. Then $\delta(T)_p$ values decrease gradually from that point. On the basis of these interpretations, the nucleation time that is necessary to achieve optimum conditions was selected as 2 h. In previous studies [10,17], it was determined that 10 K above the T_p value was sufficient for crystal growth in the microstructure of the glass sample. Therefore, crystallization temperatures were also chosen 10 K above the T_p values in this study. Consequently, maximum nucleation temperature, maximum nucleation time and crystallization temperature of ORSG glass were determined as 988 K, 2 h and 1188 K, respectively.

The same observations were detected at the DTA results of TG glass (Table 4). As seen from Table 4, T_p values decreased and $\delta(T)_p$ values increased until the temperature of 948 K for TG sample. With the increasing of nucleation time, $\delta(T)_p$ values reached a maximum at 2 h. Then $\delta(T)_p$ values decrease gradually from that point. On the basis of DTA results and the interpretations mentioned above, maximum nucleation temperature, maximum nucleation time and crystallization temperature of TG glass were determined as 948 K, 2 h and 1140 K, respectively.

An idealized heat treatment schedule for producing glass-ceramics from industrial wastes was determined with the aid of DTA results. The applied heat treatment schedules to the glasses and the codes of the produced samples were given in Table 5.

3.3. Microstructural characterization of the produced glass-ceramic samples

In order to identify the crystalline phases, XRD analysis was carried out on the produced glass-ceramic samples. Fig. 3 is the X-ray pattern of ORSGC-15 sample. X-ray diffraction analysis revealed that the main crystalline phase occurred in all ORSGC samples was diopside. $CaO–Al_2O_3–SiO_2$ (CAS) system glasses are one of the fundamental silicate systems that have been used widely in many fields of industry. The crystallization of CAS system glasses produced from industrial wastes has been investigated by many researchers and also reported that the main crystalline phases can be diopside, anorthite and wollastonite in this ternary system [3–5]. Chemical composition of ORSG samples is in the $CaO–Al_2O_3–SiO_2$ ternary glassy system. ORSG is a CAS type glass but Fe_2O_3 content of it is high enough compare to the CAS type glasses. For crystallization of CAS type glass Fe_2O_3 works efficiently as a nucleant to promote the speed of nucleation [18]. Iron oxide decreases glass

Table 5
Codes of the produced glass-ceramic samples

Glass	Nucleation stage	Crystallization stage	Code of the glass-ceramic samples
ORSG	Nucleated at 988 K for 2 h	Crystallized at 1188 K for 15 min	ORSGC-15
		Crystallized at 1188 K for 30 min	ORSGC-30
		Crystallized at 1188 K for 60 min	ORSGC-60
TG	Nucleated at 948 K for 2 h	Crystallized at 1140 K for 15 min	TGC-15
		Crystallized at 1140 K for 30 min	TGC-30
		Crystallized at 1140 K for 60 min	TGC-60

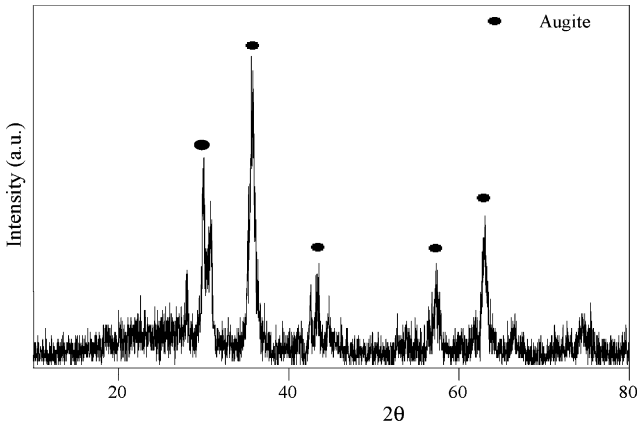

Fig. 4. XRD pattern of the TGC-60 sample.

viscosity and therefore, it increases the crystal growth rate since Fe^{3+} ion could act as a modifier of the structure, with breaking the Si–O–Si bonds [19]. When the temperature was increased further to the maximum nucleation and crystallization temperatures to produce glass-ceramics diopside phase took place in the whole body of the ORSGC samples. However, this result is quite different from the results of some other researchers who used coal fly ash as a raw material in the glass-ceramic production. They obtained anorthite, wollastonite and mullite phases in the CAS type coal fly ash-based glass-ceramics [20,21]. This phenomenon indicates the complexity and uncertainty of nucleation and crystallization in the CAS glass system.

XRD pattern of TGC-60 sample was shown in Fig. 4. XRD results revealed that the main crystalline phase was aluminum augite. The main components of TG sample are SiO_2, Al_2O_3 and Fe_2O_3. CaO and MgO contents of TG sample are lower compare to the ORSG sample. In the structure of glass, O^{2-} is attracted to near Si^{4+} in the form of $(SiO_4)^{4-}$. At the same time the network modifiers also have a tendency to attract O^{2-} with a partial negative charge (non-bridge oxygen), so the network modifiers compete with Si^{4+} for O^{2-} [22]. When the surrounding temperature is equal to T_g, the structure of the glass becomes relaxed and diffusion of ions occurs easier. For glass with more network modifiers, non-bridged oxygens are concentrated in the area that contains more network modifiers and the glass separated into two phases, which are the phase with more Si^{4+} and the phase with more network modifiers. The conditions of nucleation are that ions diffuse together from the uniform glassy matrix and the ions are rearranged to give the structure of the crystals. Although it is usually an intermediate glass network ion, the Fe^{3+} could act as a modifier of the TG glass structure, breaking the Si–O–Si bonds to form the augite phase. Mg and Ca ions have also effects on the formation of crystalline structure as network modifiers [22]. However, Fe^{3+} plays an important role in the crystalline structure as the network modifier since the content of Fe^{3+} is high enough compare to the Ca and Mg ions for TG sample. Ca and Mg contents of the ORSG sample are higher than that of the TG sample. Therefore, diopside phase occurred in the ORSG sample instead of augite phase as it was obtained in the TG sample. The formation of augite has been reported during crystallization of coal fly ashes by Barbieri et al. [5]. Moreover, augite crystals

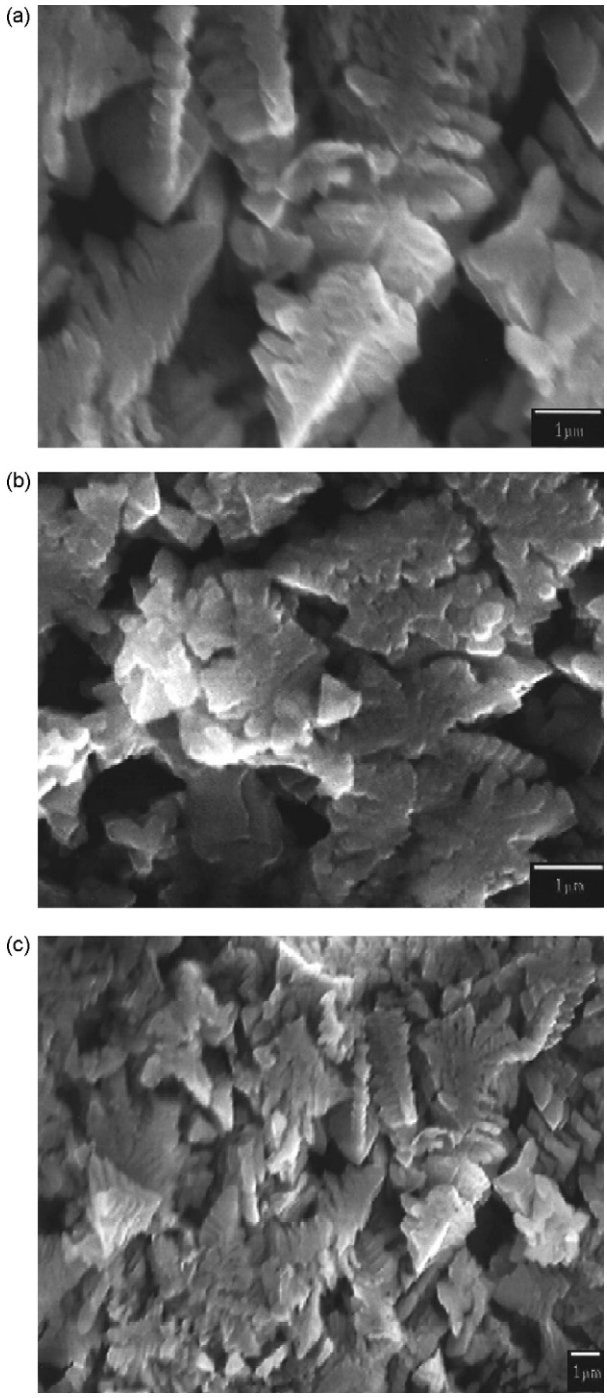

Fig. 5. SEM micrographs of ORSGC-15 (a), ORSGC-30 (b) and ORSGC-60 (c).

have also been observed in glass-ceramics obtained from other industrial wastes rich in Fe-ion such as, incinerator fly ash [23], and electric arc furnace dust(EAF) [24].

SEM investigations were conducted in order to get a better understanding of the morphology of the microstructure. SEM micrographs of ORSGC-15, ORSGC-30 and ORSGC-60 samples heat-treated at different holding times at the crystallization temperature are shown in Fig. 5. SEM observations revealed that both locally oriented dendritic crystalline growth and a significant number of leaf-shaped crystals occurred in the glass-

Table 6
Properties of the produced glass-ceramic samples

Sample name	Hardness (kg/mm^2)	Density (g/cm^3)	Porosity (%)	Water adsorption (wt.% loss)
ORSGC-15	577	2.71	1.08	0.21
ORSGC-30	711	2.82	0.96	0.14
ORSGC-60	827	2.91	0.61	Negligible
TGC-15	628	3.03	0.71	Negligible
TGC-30	776	3.14	0.17	Negligible
TGC-60	867	3.32	0.10	Negligible

ceramic samples. It was found that the volume of the crystalline phase increased after the holding time increased from 15 to 60 min, as it was seen from Fig. 5. This is due to higher driving force and increasing the crystal growth rate with the longer heat treatment process. The nuclei got more energy to achieve the crystal growth process when the holding time at crystallization temperature increased. Pelino et al. [25] reported that increasing of crystallization time has a positive effect on the properties of glass-ceramic materials and the physical and mechanical properties of them yielded better characteristics. It was also observed that some pores with irregular shapes were found in the ORSGC-15, ORSGC-30 and ORSGC-60 samples. The amount of pores decreased with the increase in the heating time. This is occurred since the number of the crystallites increased.

SEM micrographs of the TGC-15, TGC-30 and TGC-60 samples were given in Fig. 6. In all cases, SEM analyses show the presence of strongly interlocked crystals of about 100–500 nm size embedded in a glassy matrix. The morphology of the crystalline phase is composed of equiaxed or spherical networks forming a fully ordered microcrystalline mosaic that is mainly made up of augite. Microstructural observation clearly indicated that crystallization volume increases when the length of thermal treatment time increased. Fig. 6 shows the following features: some of the equiaxed nano-crystals with a bright contrast were occurred in the glassy matrix; some of the nano-crystals exhibiting a grey contrast and making the most part of the crystalline phase and; areas of the amorphous residual glassy phase which appears in dark contrast.

3.4. Physical and mechanical properties of the produced glass-ceramic samples

Table 6 gives values for the microhardness, density, porosity and water absorption of ORSGC and TG samples. The general trend in microhardness found is that as samples become more crystalline, the average microhardness increases. The hardness values found for TGC samples are greater than for ORSGC samples. The microhardness trend is consistent with what can be expected based on crystallization. The TGC samples have more crystalline sites, whereas ORSGC samples have less crystalline sites, as it was observed from the SEM micrographs. The crystalline size and the shapes of the ORSGC samples are different from the TGC samples. The crystalline size of the ORGC samples is bigger than that of TGC samples. Therefore, hardness values of ORSGC samples are lower than those of TGC samples. In compliance with the hardness values, density values of the glass-ceramic samples increased with the increase in crystallization degree. Density values of ORSGC samples are in the range of 2.71–2.91 g/cm^3. The density of diopside is 3.39 g/cm^3. Therefore, it is expected that the density of the samples increased with the increase in crystalline phase occurred in the glass-ceramic samples. ORSG-60 sample has the highest density value with the highest crystalline degree in all ORSGC samples. Densities of TGC samples are in the range of 3.03–3.32 g/cm^3 and increased with increasing crystallization degree and decreasing pore volume as it was obtained from the SEM investigations. Both porosity and water absorption values correlated well with each other and decreased with the increase of crystallinity. The porosity and water absorption values of TGC samples are lower than the ORSGC samples since the crystallization degree is higher in the TGC samples. The presence of pores in the ORSGC samples was also confirmed by SEM observations. The factors regulating physical, mechanical and chemical properties are crystalline phase, crystallization degree, the size of the crystallites and homogeneity of crystal size [20]. The closed porosity was observed in the TGC samples. The detailed SEM investigations, density and porosity values of the produced samples indicated that the TGC-60 sample had the highest crystallization degree. The closed porosity remained in the glass-ceramic samples for the shorter crystallization time damaged continuity of the crystal phase accounting for the decrease in hardness of the bulk glass-ceramic samples. TGC samples have higher crystallization degree with a smaller crystalline size and less porosity compare to ORSGC samples. It was reported that fine-grained glass-ceramics possess better properties [26]. With the increasing of crystallization degree, crystallites were strongly interlocked together to form a more dense crystalline structure and amorphous glassy phase decreased gradually. Therefore, physical and mechanical properties of TGC samples are better than the ORSGC samples.

Density and hardness values of ORSGC samples are higher than the glass-ceramic samples produced in different studies from coal fly ash and incinerator fly ash [23,26]. Porosity and water absorption values of TGC samples are lower than the values reported by Cheng et al. [27].

3.5. TCLP results of the produced glass-ceramic samples

TCLP results of the ORSGC and TGC samples are given in Table 7. Any heavy metal concentration could not be detected in the extraction solution of the TGC-15 sample. However, small concentrations of Zn ion was detected in the extraction

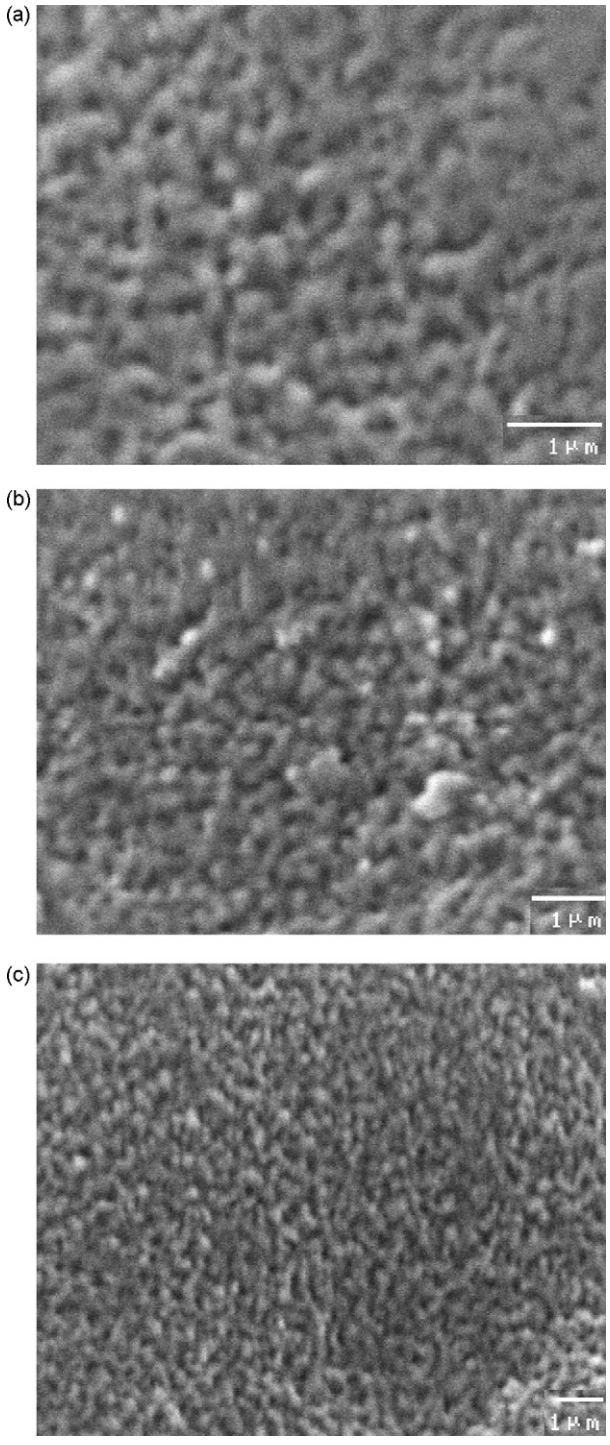

Fig. 6. SEM micrographs of TGC-15 (a), TGC-30 (b) and TGC-60 (c).

Table 7
TCLP results of the produced glass-ceramic samples

Sample name	Cr (ppm)	Mn (ppm)	Zn (ppm)	Pb (ppm)
ORSGC-30	BD	BD	0.005	BD
TGC-15	BD	BD	BD	BD

BD: below detection limit.

Table 8
Chemical resistances of the produced glass-ceramic samples

Sample name	HNO_3 (%)	NaOH (%)
ORSGC-15	0.600	Negligible
ORSGC-30	0.420	Negligible
ORSGC-60	0.280	Negligible
TGC-15	0.100	Negligible
TGC-30	0.033	Negligible
TGC-60	0.015	Negligible

solutions of the ORSGC-30 sample. But that value is still lower than the limits required by US EPA. Transformation of glass into a glass-ceramic material significantly improves the leachability characteristics of the materials since the crystalline phase remains while the residual glass is dissolved away during leaching. Heavy metal ions replaced with other ions and successfully solidified in the crystalline structure. Diopside and augite phases have been shown to be ideal crystalline matrixes for the immobilization of wastes in the production of glass-ceramic materials. TCLP results of ORSGC samples are better than the TCLP results of bulk glass-ceramics produced by Cheng [24,28] and Kavouras et al. [29]. TCLP results showed that the ORSGC and TGC samples are non-toxic materials. Consequently, the produced glass-ceramic samples were sufficiently stabilized, according to the US EPA standards.

3.6. Chemical resistance of the produced glass-ceramic samples

Table 8 shows the chemical durability of glass-ceramic materials. It can be seen that the durability of both TGC and ORSGC glass-ceramic samples correlate with volume of the crystalline phase and show acceptable chemical resistance behavior for all samples. However, comparing the chemical durability results of TGC samples with ORSGC samples, it can be seen that the weight loss percent is lower than those for the ORSGC samples in HNO_3 solution. This seems to be due to the more bonding in TGC glass-ceramics network rather than the ORSGC samples, due to the formation of crystalline phases during heat treatment process. The achievement of high chemical durability in glass-ceramics indicates that the chemical composition of the crystalline phases obtained favor good stability. McMillan [6] had stated that the glass-ceramics, in general, possess good chemical stability and that they compare favorably in this respect with other ceramic type materials. It is known that the glassy matrix is more easily leached in the acidic solutions. Studying the chemical durability of glass-ceramics revealed that the weight loss decreased with the increase in the volume crystalline content. Consequently, an increase in the content of the crystalline phase results the higher chemical resistance in the glass-ceramic materials. Therefore, chemical resistance of the TGC samples, especially of the TGC-60 sample are higher than the ORSGC samples. It is apparent that the produced glass-ceramic samples show higher resistance to alkali solutions than to the acidic solutions. Chemical resistances of glass-ceramics are better than those glass-ceramics produced

in different studies from coal fly ash and incinerator fly ash [24,28,30].

4. Conclusions

On the basis of DTA results, maximum nucleation temperature, maximum nucleation time and crystallization temperature of ORSG glass were determined as 988 K, 2 h and 1188 K, respectively, while those values for TG glass were estimated as 948 K, 2 h and 1140 K, respectively.

XRD studies revealed that the crystalline phase of TGC sample is different from the ORSGC sample's crystalline phase since the chemical composition of Tunçbilek fly ash is different from the composition of mixed wastes (Orhaneli fly ash, red mud and silica fume).

The properties of the glass-ceramic samples were influenced by the glass composition, glass production conditions and the heat treatment process. SEM observations showed that the crystalline size and the shapes of the ORSGC samples are different from the TGC samples. Nano-crystal glass-ceramics were produced from Tunçbilek fly ash without any additives by suitable heat treatment conditions.

It was also observed that the volume of the crystalline phase increased with the increase in holding time at T_p values in all glass-ceramic samples and this result caused to improve the physical, mechanical and chemical properties of the glass-ceramic samples.

Overall results indicated that coal fly ash can be used as a raw material to produce glass-ceramic materials with or without the addition of red mud and silica fume and coal fly ash-based glass-ceramics have several desirable properties that would make them attractive to industrial use in construction, tiling and cladding applications.

References

[1] C.L. Carlsson, D.C. Adriano, Environmental impacts of coal combustion residues, J. Environ. Qual. 22 (1993) 227–247.

[2] C. Leroy, M.C. Ferro, R.C.C. Monteiro, M.H.V. Fernandes, Production of glass-ceramics from coal ashes, J. Eur. Ceram. Soc. 21 (2001) 195–202.

[3] L. Barbieri, A. Corradi, I. Lancelotti, Thermal and chemical behavior of different glasses containing steel fly ash and their transformation into glass-ceramics, J. Eur. Ceram. Soc. 22 (2002) 1759–1765.

[4] A.R. Boccacini, M. Petitmermet, E. Wintermantel, Glass-ceramics from municipal incinerator fly ash, Am. Ceram. Soc. Bull. 97 (1997) 75–78.

[5] L. Barbieri, T. Manfredini, I. Queralt, J.M. Rincon, M. Romero, Vitrification of fly ash from thermal power stations, Glass Tech. 38 (1997) 165–170.

[6] P.W. McMillan, Glass-ceramics, 2nd ed., Academic Press, London, 1979.

[7] X.J. Xu, C.S. Ray, D.E. Day, Nucleation and crystallization of $Na_2O{\cdot}2CaO{\cdot}3SiO_2$ glass by DTA, J. Am. Ceram. Soc. 74 (1991) 909–914.

[8] M. Erol, S. Küçükbayrak, A. Ersoy-Meriçboyu, T. Ulubaş, Removal of Cu^{2+} and Pb^{2+} in aqueous solutions by fly ash, Environ. Conv. Manage. 46 (2005) 1319–1331.

[9] N. Karatepe, Değişik Sorbentler Yardımıyla Baca Gazlarından Kükürt Dioksit'in Giderilmesi, PhD Thesis, ITU Institute of Science and Technology, 1996.

[10] M. Erol, S. Küçükbayrak, A. Ersoy-Meriçboyu, M.L. Öveçoğlu, Crystallization behavior of glasses produced from fly ash, J. Eur. Ceram. Soc. 21 (2001) 2835–2841.

[11] US EPA, US Environmental Protection Agency Method 1311 (Reviewed), US EPA, Washington, DC, 1992.

[12] Annual Book of ASTM Standards, C-20, Standard test methods for appearent porosity, water absorption, apparent specific gravity and bulk density of burned refractory brick and shapes by boiling water, 2000.

[13] M. Erol, S. Küçükbayrak, A. Ersoy-Meriçboyu, The recycling of the coal fly ash in the glass production, J. Environ. Sci. Health, Part A 41 (2006) 1921–1929.

[14] W. Li, B.S. Mitchell, Nucleation and crystallization in calcium aluminate glasses, J. Non-Cryst. Sol. 255 (1999) 199–207.

[15] H.C. Park, S.H. Lee, B.K. Ryu, M.M. Son, I. Yasui, Nucleation and crystallization kinetics of $CaO–Al_2O_3–2SiO_2$ in powdered anorthite glass, J. Mater. Sci. 31 (1996) 4249–4253.

[16] C.S. Ray, D.E. Day, Determining the nucleation rate curve for lithium disilicate glass by DTA, J. Am. Ceram. Soc. 73 (1990) 439–442.

[17] M. Erol, A. Genç, M.L. Öveçoğlu, S. Küçükbayrak, Y. Taptık, E. Yücelen, Characterization of a glass-ceramic produced from thermal power plant fly ashes, J. Eur. Ceram. Soc. 20 (2000) 2209–2214.

[18] S. Suzuki, M. Tanaka, T. Koneko, Glass-ceramic from sewage sludge ash, J. Mater. Sci. 32 (1997) 1775–1779.

[19] L. Barbieri, A. Corradi, I. Lancelotti, A.P.N. De Oliveira, O.E. Alarcon, Nucleation and crystal growth of a $MgO–CaO–Al_2O_3–SiO_2$ glass with added steel fly ash, J. Am. Ceram. Soc. 85 (2002) 670–674.

[20] F. Peng, K. Liong, A. Hu, H. Shao, Nono-crystal glass-ceramics obtained by crystallization of vitrified coal fly ash, Fuel 83 (2004) 1973–1977.

[21] L. Barbieri, I. Lancelotti, T. Manfredini, G.C. Pellaconi, J.M. Rincon, M. Romero, Nucleation and crystallization of new glasses from fly ash originating from thermal power plants, J. Am. Ceram. Soc. 84 (2001) 1851–1858.

[22] M. Sivasundaram, Glass-ceramics from pulp and paper waste ash, MSc Thesis, Department of Mining and Metallurgical Engineering, McGill University, Canada, 2000.

[23] M. Romero, R.D. Rawlings, J.M. Rincon, Development of a new glass-ceramic by means of controlled vitrification and crystallization of inorganic wastes from urban incineration, J. Eur. Ceram. Soc. 19 (1999) 2049–2058.

[24] T.W. Cheng, Combined glassification of EAF dust and incinerator fly ash, Chemosphere 50 (2003) 47–51.

[25] M. Pelino, C. Cantalini, J.M. Rincon, Preparation and properties of glass-ceramic materials obtained by recycling geothite industrial waste, J. Mater. Sci. 32 (1997) 4655–4660.

[26] F. Peng, K. Liang, A. Hu, Nano-crystal glass-ceramics obtained from high alumina coal fly ash, Fuel 84 (2005) 341–346.

[27] T.W. Cheng, T.H. Ueng, Y.S. Chen, J.P. Chiu, Production of glass-ceramic from incinerator fly ash, Ceram. Int. 28 (2002) 779–783.

[28] T.W. Cheng, Effect of additional materials on the properties of glass-ceramic produced from incinerator fly ashes, Chemosphere 56 (2004) 127–131.

[29] P. Kavouras, G. Kaimakamis, Th.A. Ioannidis, Th. Kehagias, Ph. Komniou, Kokkou, E. Pavlidou, I. Antonopoulos, M. Sofoniou, A. Zouboulis, C.P. Hadjiantoniou, G. Nouet, A. Prakouras, Th. Karakostas, Vitrification of lead-rich solid ashes from incineration of hazardous industrial wastes, Waste Manage. 23 (2003) 361–371.

[30] A. Karamanov, G. Taglieri, M. Pelino, Iron rich sintered glass-ceramics from industrial wastes, J. Am. Ceram. Soc. 82 (1998) 3006–3012.